PROCEEDINGS OF SCIENCE

LS I +61°303 is a Be-Pulsar binary, not a Microquasar

Vivek Dhawan*, **Amy Mioduszewski, & Michael Rupen**

National Radio Astronomy Observatory, Socorro, NM 87801, USA †

E-mail: vdhawan@aoc.nrao.edu, amiodusz@aoc.nrao.edu, mrupen@aoc.nrao.edu

LS I +61°303 is an HMXB discovered as a γ-ray emitter 30 years ago, and well known as a radio, X ray, and most recently a TeV source. Despite the wealth of data, the choice between pulsar and microquasar emission models remained unclear. Here we report on AU-scale radio imaging with the VLBA, that literally resolves the issue in favour of the pulsar mechanism.

Our sequence of 10 images were spaced 3 days apart and covered more than one full orbital period of 26.5 days. We observed for 5 hours per day with simultaneous reception at λ 13 cm and 3.6 cm. We show that: (i) The radio emission is resolved on scales of 2AU, and appears cometary, with the 'tail' pointed away from the high-mass star. (ii) The morphology varies dramatically near periastron, with outflow velocities $\sim$7500 km/s, and gradually around the rest of the orbit, v$<$1000 km/s at apastron. This variation is easily explained by the geometry of the eccentric orbit, rather than a precessing jet. (iii) Comparing simultaneous 13 cm and 3.6 cm images, a synchrotron opacity gradient exists along the cometary tail, with the highest-energy particles located in the head. No bulk relativistic motion is seen during any phase of the orbit.
We conclude that the pulsar model is strongly supported, i.e., the radio synchrotron emission arises not in a jet, but from particles shock-accelerated in the interaction of the pulsar wind with the dense equatorial wind from the Be star.

Astrometric accuracy of $<$0.1 milliarcsec in these observations, combined with re-processed archival data, constrains the long-term proper motion of the binary over 14 years. We show that it has a low velocity $\sim$10 km/s relative to star-forming regions W3 (IC 1795) and W4 (IC 1805) in the Perseus arm, and was not ejected at 27 km/s by the supernova event, as previously believed. We also show that the centroid of the radio emission varies during the orbit, with both systematic and random components of $\sim$1mas, obscuring the parallax (0.5mas), and the semi-major axis of the binary (0.25mas).

Finally, as a general comment, we note that radio synchrotron emission from X ray binaries may be manifest on AU scales as pulsar wind nebulae or shells, besides the often-invoked jet morphology. The latter two are low-power analogs of SNR and GRB's respectively.

VI Microquasar Workshop: Microquasars and Beyond
September 18-22, 2006
Como, Italy

*Speaker.

†NRAO is a facility of the National Science Foundation operated under cooperative agreement by Associated Universities, Inc.

PoS(MQW6)052

1. Introduction and Background

Shortly after the discovery of LS I +61°303 at 70MeV by the COS-B satellite, Gregory & Taylor [8] reported variability at 5GHz, and suggested a jet origin for the radio emission. Orbital parameters from optical spectroscopy [4] show the object to be a high mass binary: a 1-3$M_\odot$ NS or BH orbiting a Be star of $\sim$12.5$M_\odot$ with eccentricity e=0.7, and the same period of 26.496d as the radio variability. Competing models were constructed for the broadband spectra, assuming a rotation-powered pulsar insead of an accretion-powered jet, and, despite panchromatic study over the past 30 years, consensus had not emerged [17]. Incidentally, SS 433 was found in the same 5GHz survey and is an undisputed microquasar of the same vintage.

2. Emission Mechanisms

Two alternatives have been explored to fit the radio to TeV emission of the so-called γ-ray binaries LS 5039, LS I +61°303 and PSR B1959-63: accretion-powered relativistic jets, and rotation-powered pulsar wind nebulae. These models are reviewed by Mirabel [17] and are discussed briefly here.

2.1 Microquasar models

Several researchers have developed jet models based on relativistic outflow of leptonic ($e^\pm$) [3, 9, 2], and hadronic plasma [20], although these are not mutually exclusive. The radio emission is a solid fact, but the reported morphology and outflow velocites have considerable variance, e.g. Peracaula et al. [19] imaged a slowly expanding bubble, while Massi et al [14, 15], using the European radio arrays Merlin and EVN, claimed a tentative detection of large-scale, ($\sim$100AU) relativistic, precessing outflow.

Simultaneous X rays and radio monitoring by Harrison et al. [11] showed that the X rays peak near periastron, and the radio about 0.5 cycle later. This anticorrelation argues against the jet model, but does not rule it out, as there could be a delay between accretion and jet output. However, the soft X rays are relatively weak and there is little other evidence of accretion. Nevertheless, Gregory and Neish [7] discovered a $\sim$4-year radio modulation, and explained it in terms of variable accretion from the equatorial wind surrounding the Be star.

2.2 Pulsar models

In the alternate model, discussed, e.g., by Harrison, [11], Leahy, [12], and Dubus [6], a 'standard' pulsar of period $\sim$0.1s, with energy loss rate of $\sim 10^{35}$erg/s, generates the pair plasma that inflates a pulsar wind nebula of sub-AU size. The PWN expands and shocks as it interacts with the outflows from the Be star, namely, the fast polar wind, and the slow, dense equatorial wind. Emission with a non-thermal power-law spectrum from radio to keV is by the synchrotron process, and the stellar UV photons are Compton scattered up to TeV energies. A variation on this model is proposed by Chernyakova et al. [5] who fit the radio with synchrotron emission, the X ray with inverse Compton, and then invoke p-p interactions to fit the highest TeV energies.

A potential objection to the pulsar model is the lack of X ray or radio pulses, despite quite sensitive searches. This objection is removed by the discovery of the γ-ray binary PSR B1259-63,

a radio pulsar orbiting a Be star with much longer period, in which the pulsation is suppressed at periastron by the dense wind.

A recent detection of TeV photons from LS I +61°303 was reported by the MAGIC collaboration, [1], at the same orbital phase as the maximum 2cm emission monitored simultaneously with the Ryle Telescope. This observation supports the jet model as the common cause. It is yet unclear to us how this result may be accomodated in the pulsar model.

3. Our Observations.

3.1 Motivation from Previous Studies

Astrometric observations of LS I +61°303 were conducted by Lestrade [13], who found a significant proper motion. Based on these data, Mirabel et al. [18] developed an evolutionary scenario for the binary, i.e., its ejection from the star cluster IC 1805 as a result of the velocity imparted by the supernova.

3.2 New VLBA Observations

In the past two years, we have undertaken the VLBA astrometry of several X ray binaries, aimed at determining the parallax and proper motions. For LS I +61°303 we found anomalous position and morphological changes on 6-month timescales, and investigated these further with a sequence of VLBA images spaced 3 days apart, covering more than one orbit. These are the topic of the present paper.

The light curves in Fig.1 show the recent flux density variations of LS I +61°303 at 2cm, monitored by Guy Pooley with the Ryle Telescope till MJD 53905. The last 10 points, MJD 53917-947, are VLBA total flux measurements from our sequence of images at 3.6cm (Fig.3). The lower panel in Fig.1 shows two different pieces of the 3.6cm archive of GBI data from several years ago, demonstrating both the weak and strong variability of the basic 26.5-day cycle. Our recent data are typical for the source in its weaker state. Gregory & Neish [7] explained the modulation of the radio cycles as variable accretion in a disk wind. This may need re-examination in the context of the pulsar wind scenario.

3.2.1 Images

The set of images at 3.6cm are shown in Fig.3. The orbital phase at top left of each image is computed according to Gregory,[7] and Casares [4]. Periastron is at 0.23. Smaller font indicates the two images from Dec.2004 and Oct.2005, inserted at appropriate orbital phase. The other 10 images are from the July 2006 time sequence which sampled two periastron passages.

Comparing images 3 days apart, it is clear that rapid changes are seen in the orientation of the cometary tail at periastron. The length of the tail (6.5mas) corresponds to an outflow velocity at least 7500km/s, 0.025 c, assuming $\sim$3 days to fill the tail. (Assuming 1 day, v$\sim$0.075 c. While much lower than the 0.6 c assumed by some authors, our measurements are compatible with 0.1 c, expected for an over-pressured PWN, suggested by Chernyakova et al.). No extended features or higher velocities were detected on any days. At other phases the tail is amorphous. The shift of centroid from day to day gives $\sim$1800 km/s max, with 1000 km/s typical. For comparison, v_{max} of the pulsar in the orbit is 300km/s.

The images at 13cm have lower resolution of 8 AU. Generally the same features are seen as at 3.6cm, except: (i) Flux density peaks later in the orbital cycle; (ii) There is less variation; (iii) the peak intensity in each image is further displaced radially outward from the pulsar orbit, and lags by a few days in time. These effects can be ascribed to a density (or optical depth) gradient along the cometary tail i.e. synchrotron self-absorption. The most rapid position shifts in the centroid (1.3mas/day) are again seen at periastron, with corresponding v 4500km/s. See also the caption to Fig.4.

Next we examined the pairs of images from half of the 5 hours of data on each day. The changes are generally small, and any flow velocity cannot exceed 5% of c. Near periastron, a rotation of the inner structure is apparent, in the same sense (counterclockwise) and at the same rate, as the images taken 3 days apart, i.e. roughly 5-7° in 2.5hrs, or ∼60°/day.

We next searched for large-scale outflows. In archival data for 48 continuous hours, taken by Taylor et al in 1999, and re-processed by us, we confirm that low velocities of ∼1000 km/s, as reported by [19], are present in the subsets of 5hr duration. Integrating over the whole dataset, which included the world's largest radio telescopes, no halos or outflows larger than 5 mas were detectable down to rms of 25μJy. Similarly, in the subset of data from the 27-element VLA phased array, no structure was detected outside 200 mas, down to a level of 17μJy. These data were taken at 6cm, near apastron, when the source was unusually strong and could be self-calibrated to give deep images.

3.2.2 Astrometry

All our observations were phase-referenced to a pair of calibrators with ICRF positions, and the results are consistent within 0.1 mas over all the recent images. We also re-processed, with somewhat lower precision, archival data [19], and updated the position of Lestrade for the shift in reference catalog used by the VLBA. The result is shown in Fig.2, with details in the figure caption.

In summary, our long-term measurement of the proper motion shows it to be slower than the previous result, which was very likely affected by orbital motion and random changes in the turbulent outflow, as seen in Fig.4.

3.2.3 Space velocity and SN mass loss.

In this section (see Table-1), we update the runaway binary scenario proposed in [18], as follows: (i) The new VLBA proper motion is 4 km/s, compared to 17 km/s before. (ii) The radial velocity for LS I +61°303 is from [4], about 14 km/s change. (iii) The distance to LS I +61°303 is set to 2.0 kpc, from new VLBA parallax distances to W3OH (see Table-1). Changing 2 to 2.3 kpc has little effect. (iv) The LSR conversion assumes a peculiar Solar$_{UVW}$ of (+10, +5.25, +7.17) from Dehnen & Binney 1998, based on Hipparcos data. Previously the accepted value was (+9, +12, +7).

The result is that LS I +61°303 is not a runaway from the massive star-forming regions in the Perseus arm. The motion is about 10km/s, with errors from variations in the motion of gas as traced by the masers (7km/s for water masers [10], 2km/s for methanol masers, [22].) The low velocity, following [21, 18], implies a loss of only ∼1M$_\odot$ in the SN event, and, moreover, the high eccentricity implies an asymmetric kick from the SN to the pulsar.

	V_{Radial}	PM_{RA} mas/yr	PM_{DEC}	D kpc	U km/s	V km/s	W km/s
1	-48.0±1	-1.204±0.02	-0.147±0.01	1.95±0.04	50.5±0.7	-22.5±0.7	1.0±0.2
2	-40.2±2	-0.302±0.07	-0.257±0.05	2.00±0.10	39.8±1.5	-21.6±1.5	3.0±0.6
3	-41.2±3	-1.020±0.40	-0.880±0.40	2.00±0.10	43.0±3.4	-19.8±3.4	-4.9±3.8

Table 1: The velocity discrepancy between LS I +61°303 (item 2) and nearby star-forming regions (1 & 3), is about 10 km/s. (1) l=133.95, b=1.06 W3OH = IC 1795, methanol masers, 12.2GHz [22]. (2) l=135.68, b=1.09 LS I +61°303, Dhawan et al 2006; V_{rad} [4]. (3) l=134.72, b=0.92 IC 1805 = W4, [18] updated with D=2kpc.

4. Conclusions

VLBA imaging over a full orbit of LS I +61°303 shows that:

1. The emission is resolved on scales of 1mas (2AU), and appears cometary, pointed away from the high-mass star. No relativistic motion, nor halos, nor large-scale structures, are detectable at any phase of the orbit, nor in deeper images at apastron. It is a pulsar wind nebula shaped by the anisotropic environment, not a jet.

2. The morphology varies dramatically at periastron, and gradually around the rest of the orbit. Outflow velocity V$\sim$7500 km/s is estimated near periastron, reducing gradually to V $\sim$1000 km/s near apastron.

3. Comparing 3.6 and 13cm images, there is a synchrotron opacity gradient along the tail.

4. The radio light curve (flares a few days after periastron) may be explained as an increase in flux occurring during the near side of the orbit, when the tail is seen unabsorbed by the head. It remains to be seen if this picture is compatible with pulsar-based models for X ray, γ-ray, TeV, lightcurves.

5. Astrometry with <0.1mas accuracy shows that the cometary head traces an erratic ellipse, of semi-major axis 1.5AU, about 4 times the binary axis. The parallax (0.5mas) is totally masked.

6. The binary has a low space velocity relative to its birthplace in the Perseus arm, implying a loss of only about $\sim 1 M_{\odot}$ in the SN event.

7. It should be possible to refine the properties inferred for the pulsar wind nebula and the Be wind, based on the radio images. In particular, the lack of any structures larger than about 10AU should help constrain the relative cooling times for synchrotron, Compton and adiabatic expansion processes.

As a final remark, we note that radio emission from XRB's can assume the shape of pulsar wind nebulae, as in the present case; or shell remnants as in the case of CI Cam [16]; apart from the more usual jets. The latter 2 may be low-power (10^{-9}) analogs of SNR and GRB. Radio imaging on AU scales is the only sure way to tell the difference.

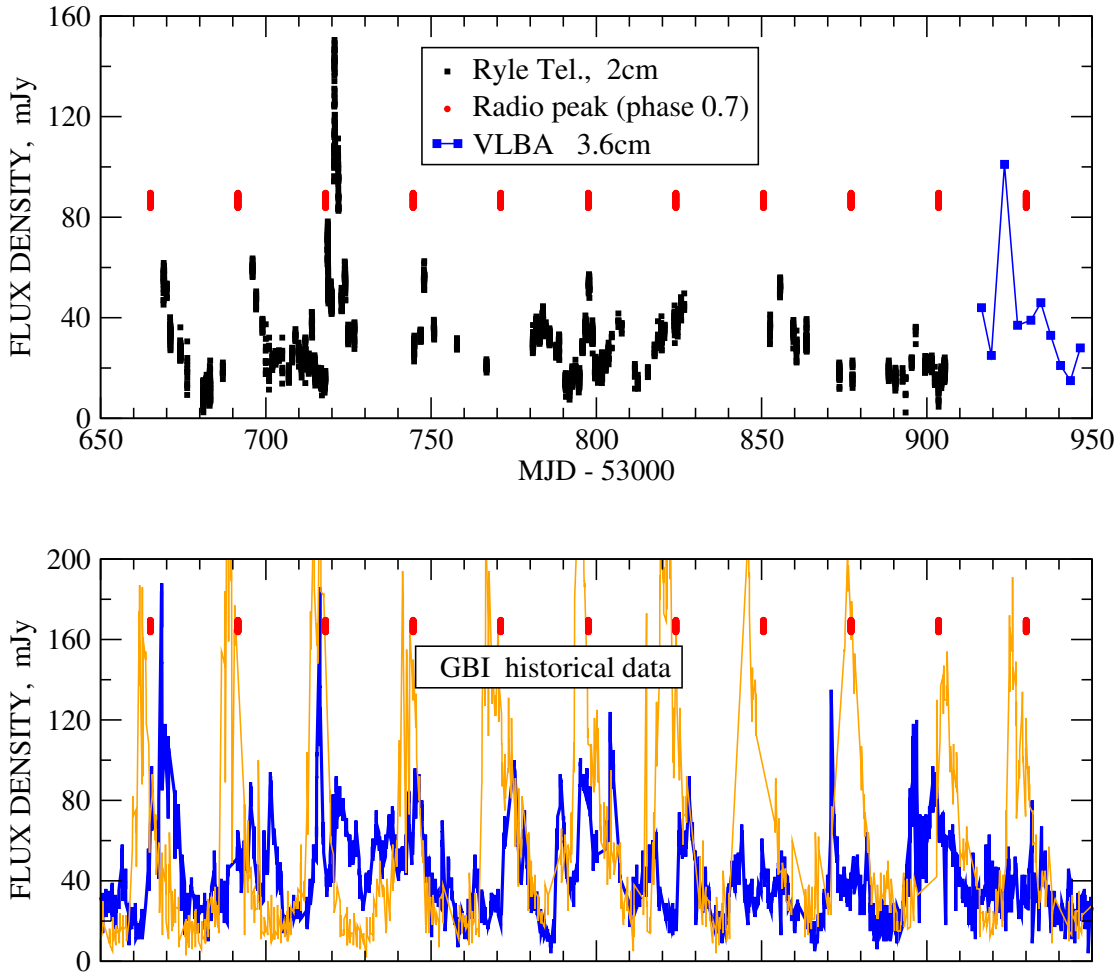

Figure 1: **Top panel** shows the recent flux density variations of LS I +61°303 at 2cm, from the Ryle Telescope. The last 10 points are from our images at 3.6cm (see Fig.3). The short vertical (red) bars show the phase of 0.7 where the radio peaks on average. **Bottom panel** shows two separate pieces, both from the 3.6cm archive of GBI data from several years ago, demonstrating both the weak and strong variability of the basic 26.5-day cycle. Our recent data are typical for the source in its weaker state. The cycle observed by Albert et al [1] is the one with peak at MJD 53800.

References

[1] J. Albert, et al. *Variable Very-High-Energy Gamma-Ray Emission from the Microquasar LS I +61° 303*, Science **312**, 1771–1773 (2006) [astro-ph/0605549].

[2] W. Bednarek, *Inverse Compton $e^{+/-}$ pair cascade model for the γ-ray production in massive binary LS I +61°303* , MNRAS **371**, 1737–1743 (2006) [astro-ph/0606421].

[3] V. Bosch-Ramon and J. M. Paredes, *γ-ray emission from microquasars: A numerical model for LS I +61°303*, A&A **425**, 1069–1074 (2004) [astro-ph/0407016].

[4] J. Casares, I. Ribas, J. M. Paredes, J. Martí, and C. Allende Prieto, *Orbital parameters of the microquasar LS I +61°303*, MNRAS **360**, 1105–1109 (2005) [astro-ph/0504332].

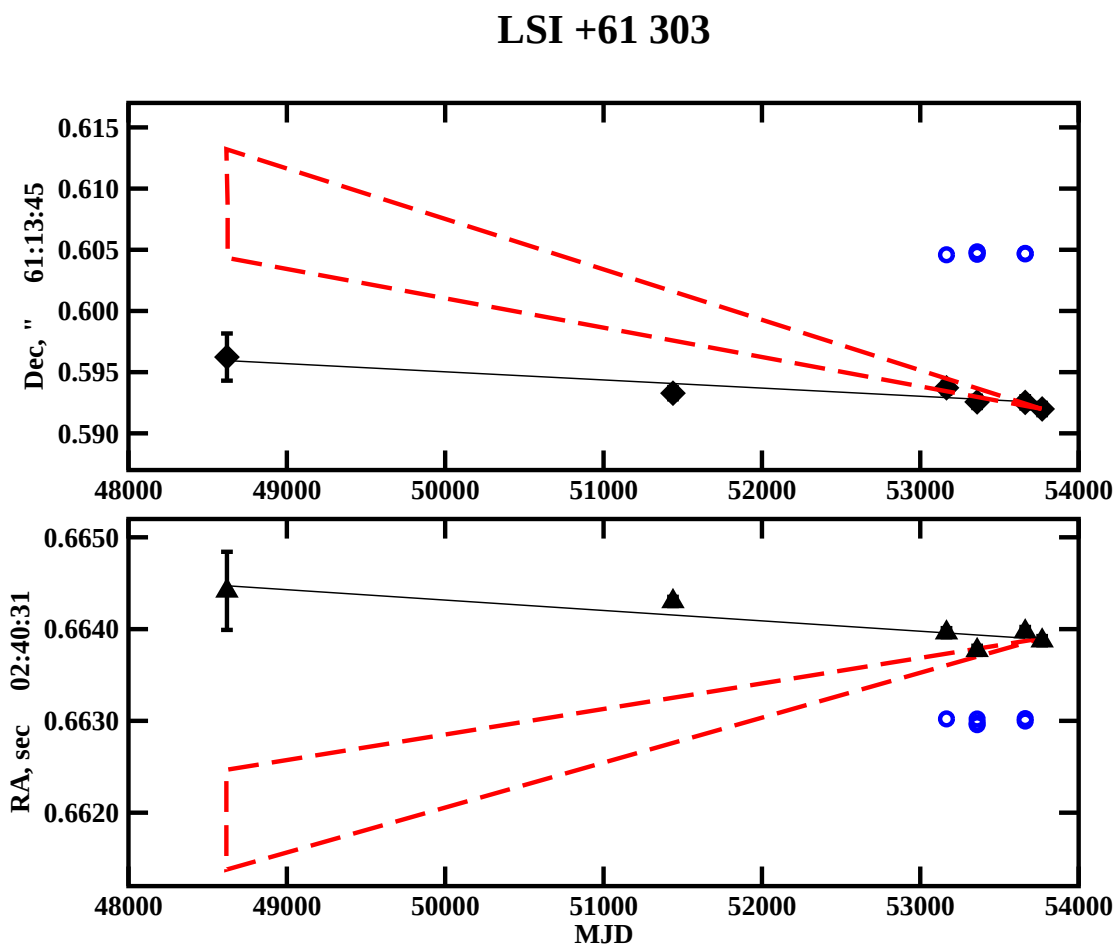

Figure 2: Astrometric positions over a timespan of 14 years, convered to a common reference frame. The leftmost point is from Lestrade 1999 (who measured position and proper motion). The central point is archival VLBA data reprocessed to get the astrometry. The right points are our recent data. The dashed (red) lines shows the proper motion of Lestrade, including errors, projected backward from a recent point. It is clear that (i) the old proper motion is not compatible with the new fit (thin line). (ii) In the short term, the position changes of the source may have affected Lestrade's determination of the proper motion. This is clarified in Fig.4, where we show that the position is modulated by the orbital phase. The circle (blue) symbols mark a second extragalactic calibrator about 1° away which was observed simultaneously to estimate the errors.

[5] M. Chernyakova, A. Neronov, and R. Walter, *INTEGRAL and XMM-Newton observations of LS I +61°303*, MNRAS, 1051–+ (2006) [astro-ph/0606070].

[6] G. Dubus, *Gamma-ray binaries: pulsars in disguise?*, A&A **456**, 801–817 (2006) [astro-ph/0605287].

[7] P. C. Gregory and C. Neish, *Density and Velocity Structure of the Be Star Equatorial Disk in the Binary LS I +61°303, a Probable Microquasar*, ApJ **580**, 1133–1148 (2002).

[8] P. C. Gregory and A. R. Taylor, *New highly variable radio source, possible counterpart of gamma-ray source CG135+1*, Nature **272**, 704–706 (1978).

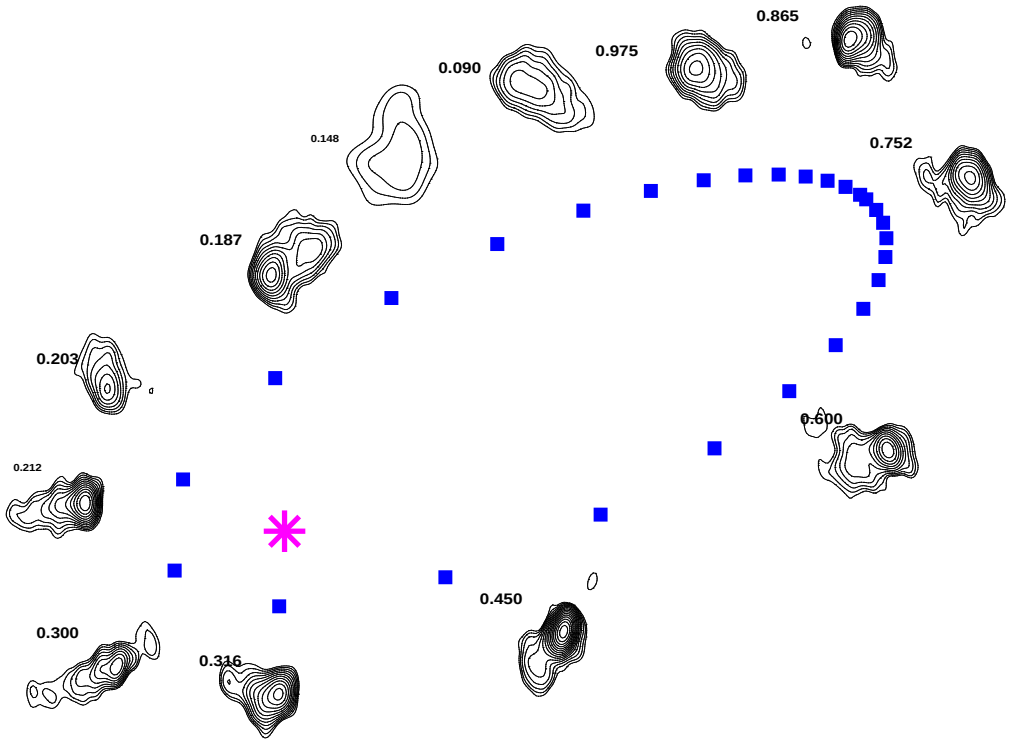

Figure 3: Images at 3.6cm arranged by orbital phase φ. Contours begin at $\pm$0.2mJy, and step by a factor $\sqrt{2}$. The resolution is 1.5x1.1 mas = 3x2.2 AU. The image locations have been adjusted for non-overlap, and are hence approximate and illustrative only. Orbit size is greatly exaggerated. Astrometric positions and orbit are displayed to correct scale in Fig.4. The squares show the locations of the pulsar 1 day apart ($\Delta\varphi$ = 0.0377), with periastron at extreme left (φ=0.23). The time progression is counter-clockwise. The ellipse is projected with parameters from Casares et al 2005, and inclination 60°, appropriate for pulsar mass 1.4$M_{\odot}$. Note the cometary tail pointed away from the high-mass Be star; the diffuse emission trailing in the wake of the pulsar; the rapid changes at periastron; and the more compact, brighter emission on the near side ($\varphi \sim$0.5) compared to the far side ($\varphi \sim$0).

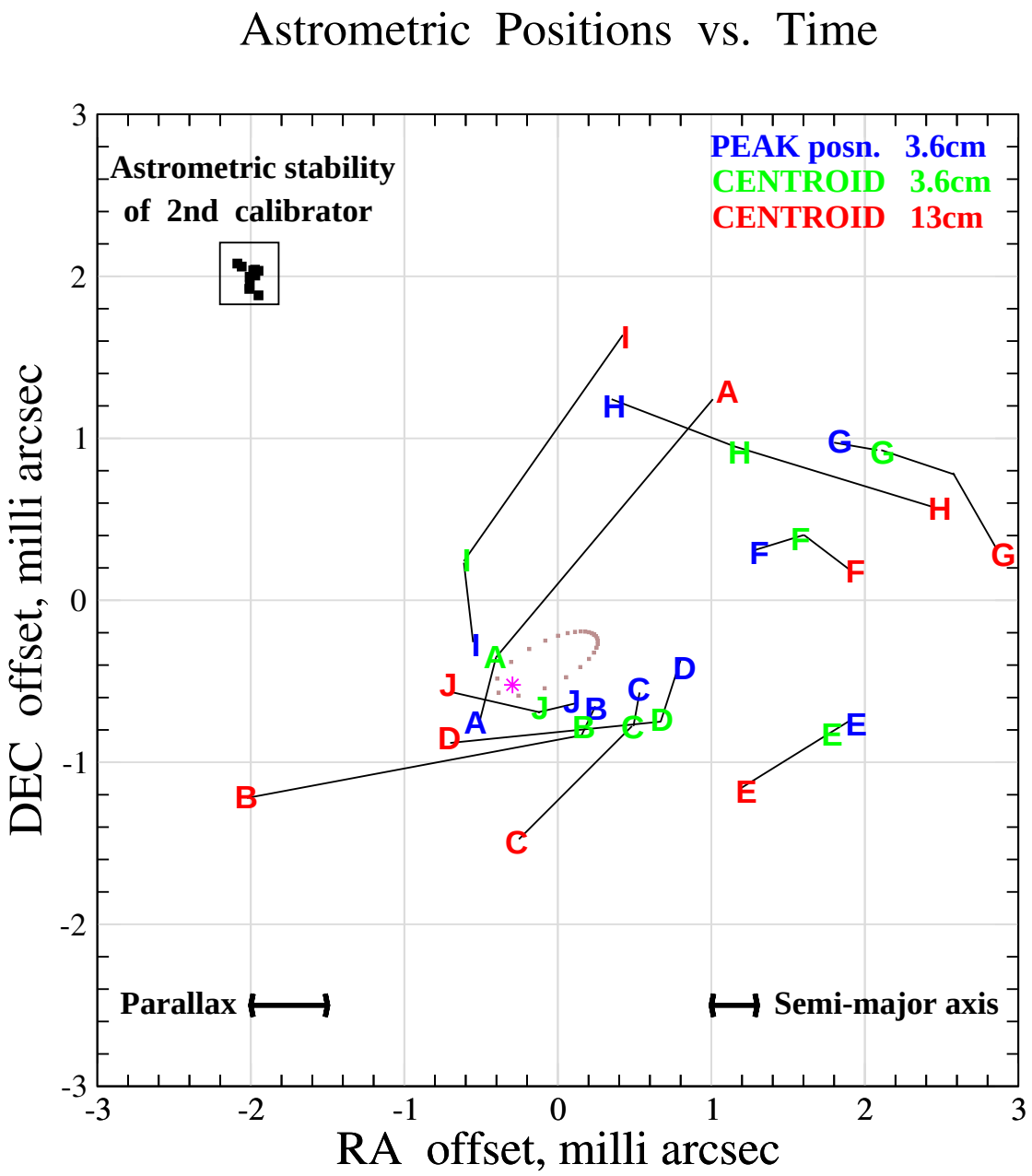

Figure 4: The letters A-J denote the time sequence, with 'A' corresponding to the image with phase =0.187, 'B'=0.300, etc., from Fig.3. The location of the letter is the measured ICRF position of the centroid (green) or peak (blue) at 3.6cm. The centroids are located away from the Be star, downstream of the peak positions. The brown dots are 1 day apart, tracing an ellipse of axis 0.5 AU expected for the orbit. The location of the ellipse relative to the measurements is uncertain. The letters describe an erratic ellipse, almost 4 times larger than the orbit, and with a random component. Thus, the emission is tracing not the pulsar itself, but the place downstream in the cometary tail where synchrotron opacity $\sim$1 at λ3.6cm. The λ13cm positions (red) trace an even larger ellipse, and lag behind by a few days compared to 3.6cm, as can be seen by the lines connecting a given letter. Hence the opacity has a gradient along the tail.

[9] S. Gupta and M. Böttcher, *A Time-dependent Leptonic Model for Microquasar Jets: Application to LS I +61 303*, ApJ **650**, L123–L126 (2006) [astro-ph/0606590].

[10] K. Hachisuka, A. Brunthaler, K. M. Menten, M. J. Reid, H. Imai, Y. Hagiwara, M. Miyoshi, S. Horiuchi, and T. Sasao, *Water Maser Motions in W3(OH) and a Determination of Its Distance*, ApJ **645**, 337–344 (2006) [astro-ph/0512226].

[11] F. A. Harrison, P. S. Ray, D. A. Leahy, E. B. Waltman, and G. G. Pooley, *Simultaneous X Ray and Radio Monitoring of the Unusual Binary LS I +61°303: Measurements of the Light Curve and High-Energy Spectrum*, ApJ **528**, 454–461 (2000) [astro-ph/9908076].

[12] D. A. Leahy, *The gamma-ray source LS I +61°303 II. Multiwavelength emission model*, A&A **413**, 1019–1028 (2004).

[13] J.-F. Lestrade, R. A. Preston, and Jones, D. L., et al. *High-precision VLBI astrometry of radio-emitting stars*, A&A **344**, 1014–1026 (1999).

[14] M. Massi, *LS I +61°303 in the context of microquasars*, A&A **422**, 267–270 (2004) [astro-ph/0404605].

[15] M. Massi, M. Ribó, and Paredes, J. M., et al. *Hints for a fast precessing relativistic radio jet in LS I +61°303*, A&A **414**, L1–L4 (2004) [astro-ph/0312091].

[16] A. J. Mioduszewski and M. P. Rupen, *CI Camelopardalis: A Shell-shocked X Ray Nova*, ApJ **615**, 432–443 (2004) [astro-ph/0407277].

[17] I. F. Mirabel, *Very Energetic Gamma-Rays from Microquasars and Binary Pulsars* (2006) [astro-ph/0606393].

[18] I. F. Mirabel, I. Rodrigues, and Q. Z. Liu, *A microquasar shot out from its birth place*, A&A **422**, L29–L32 (2004) [astro-ph/0408562].

[19] M. Peracaula, J. M. Paredes, A. R. Taylor, S. M. Dougherty, and W. K. Scott, *VSOP Observations of the X Ray Binary LS I +61°303*, Astrophysics and Space Science Supplement **276**, 123–124 (2001).

[20] G. E. Romero, H. R. Christiansen, and M. Orellana, *Hadronic High-Energy Gamma-Ray Emission from the Microquasar LS I +61°303*, ApJ **632**, 1093–1098 (2005) [astro-ph/0506735].

[21] E. P. J. van den Heuvel, S. F. Portegies Zwart, D. Bhattacharya, and L. Kaper, *On the origin of the difference between the runaway velocities of the OB-supergiant X ray binaries and the Be/X ray binaries*, A&A **364**, 563–572 (2000) [astro-ph/0005245].

[22] Y. Xu, M. J. Reid, X. W. Zheng, and K. M. Menten, *The Distance to the Perseus Spiral Arm in the Milky Way*, Science **311**, 54–57 (2006) [astro-ph/0512223].